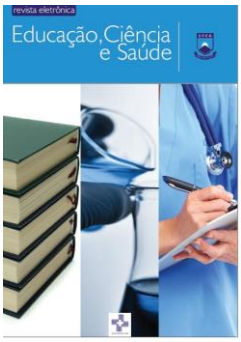

EDUCAÇÃO CIÊNCIA E SAÚDE
http://dx.doi.org/10.20438/ecs.v4i1.95

A QUANTUM BIOCHEMICAL STUDY ON OPTOELECTRONIC AND VIBRATIONAL PROPERTIES OF THE PERIPHERAL INHIBITOR L-α-METHYLDOPA HYDRAZINE

Djardiel da Silva Gomes [1], José Diêgo Marques de Lima [1], Nilton Ferreira Frazão[2], Ricardo Gondim Sarmento[3]

[1] Curso de Licenciatura em Física, Unidade Acadêmica de Física e Matemática, Universidade Federal de Campina Grande, Cuité-PB, Brazil.
[2] Prof. Unidade Acadêmica de Física e Matemática, Universidade Federal de Campina Grande, Cuité, PB, Brazil.
[3] Prof. Departamento de Ciências Biológicas, Universidade Federal do Piauí, Floriano, PI, Brazil.
Email for correspondence: nilton.frazao@ufcg.edu.br

Resumo

L-α-metildopa hidrazina (Carbidopa ou CDOPA) é um inibidor periférico de DOPA Decarboxilase (DDC) que é administrado em conjunto com a levodopa, sendo este o fármaco antiparkinsoniano mais utilizado ultimamente. Os cálculos de annealing foram utilizados para explorar o espaço da geometria molecular da carbidopa, com o objetivo de obter suas conciliações mais estáveis de menores energias, usando a teoria funcional da densidade (DFT) com os funcionais LDA/PWC, GGA/PBE e GGA/BLYP. O estudo do orbital molecular da carbidopa (HOMO, LUMO, PDOS e DOS) é obtido por uma das suas conformações de menor energia. Uma interpretação detalhada das frequências de vibração harmônica de carbidopa também é apresentada, através da análise de espectroscopia no infravermelho (IR) e por espalhamento Raman.

Palavras-chave: fármaco antiparkinsoniano, teoria do funcional da densidade, propriedades optoeletrônicas, IR e espalhamento Raman.

Abstract

L-α-methyldopa hydrazine (Carbidopa or CDOPA) is a peripheral inhibitor of DOPA Decarboxylase (DDC) that is ingested in conjunction with the levodopa, being the antiparkinsonian drug most used latterly. Annealing calculations were employed to explore the space of the molecular geometry of carbidopa, with the view to obtain its most stable conformations of smaller energies, by using density functional theory (DFT) with the LDA/PWC, GGA/PBE, and GGA/BLYP functionals. The carbidopa's molecular orbital study (HOMO, LUMO, PDOS, and DOS) are then obtained for the sake of one of its conformation of smallest energy. A detailed interpretation of the carbidopa harmonic vibrational frequencies are also presented, through the analysis of its infrared (IR) and Raman scattering spectroscopy.

Keywords: antiparkinsonian drug, density functional theory, optoelectronic properties, IR and Raman scattering.

1 Introduction

Parkinson's disease (PD) is the most common progressive, neurodegenerative disorder of the extrapyramidal nervous system characterized by the loss of nigrostriatal dopaminergic neurons (dopamine), which affects the mobility and control of the skeletal muscular system (LLOYD et al., 1970; ABOU-SLEIMAN, et al., 2006). This condition causes tremor, muscle stiffness, slowness of movement (bradykinesia) and loss balance.

Although extremely necessary, unfortunately the dopamine cannot be ingested directly by the patients, because their blood-brain barrier (BBB) do not allow its cross transport into the brain. One effective way to overcome this problem is to consider alternatively the administration of the oral dopamine precursor levodopa, which is capable of BBB crossing and it is converted into dopamine by the enzyme DOPA decarboxylase, mainly to patients at the initial stages of the disease (SCHAPIRA, et al., 2006).

Levodopa is usually administered in combination with the L-α- methyldopa hydrazine (Carbidopa or CDOPA), chemically known as (2S)-3-(3,4-dihydroxyphenyl)-2-hydrazinyl-2-methylpropanoic acid, whose chemical formula is C10H16N2O5 (CALNE, 1993). Carbidopa prevents the breakdown of levodopa in the bloodstream, and also delays its conversion into dopamine until it reaches the brain, reducing adverse side effects (HUTTON, et al., 1988). Furthermore, it can decrease peripheral aromatic L-amino acid decarboxylase (AADC) before it cross the BBB, metabolized by an enzymatic reaction of levodopa, resulting in a greater amount of levodopa dose to be transported to the brain to compensate the deficiency of dopamine and to avoid the exposure of the brain dopamine receptors to its alternating low and high concentration.

Aiming to give a quantum chemistry theoretical support to attempt in developing levodopa preparations, which may provide more continuous dopamine stimulation and less side efects; recently we presented a computational study of the levodopa adsorption on C60 fullerene at the 2-8 pH range looking for a biomedical applications to enhance the drug delivery (FRAZÃO, et al., 2012). In this study our focus is on the carbidopa molecule

since, although it occupies a prominent place in current treatment protocols as an antiparksonian drug, few works were done so far to characterize its physical properties. To fill this gap, a quantum chemistry theoretical study is presented to describe its geometrical, optoelectronic, and vibrational spectroscopic properties.

2 Materials and methods

To perform the quantum optimization, together with the optical and electronic calculations of the carbidopa, we have used the DMol3 code (DELLEY, 2000) within the density functional theory (DFT) formalism (HOHENBERG, et al., 1964; KOHN, et al., 1965) considering the local density approximation (LDA) (JONES, et al., 1989), and the generalized gradient approximation (GGA) (DAL CORSO, et al., 1996) as the exchange-correlation functionals. The LDA functional was used in its standard parametrization, as proposed by Perdew and Wang (PWC functional) (PERDEW, et al., 1992), while the GGA functional (PERDEW, et al., 1986) was taking into account using the Perdew-Burke-Ernzerhof (PBE functional) method (PERDEW, et al., 1996), as well as the BLYP functional (BECKE, 1988; BECKE, 1993). We do not adopted any pseudopotential calculation (HENRIQUES, et al., 2015; FRAZÃO, et al., 2016) to replace the core electrons in each atomic species: all electrons were included in the calculation. Double numerical plus polarization basis set (DNP) was adopted to expand the Kohn-Sham electronic eigenstates with an orbital cutoff radius of 3.5 Å.

The optimized structural parameters were used in the vibrational frequency calculations to characterize all stationary points as minima. We have utilized the gradient corrected DFT (HOHENBERG, et al., 1964) with the three-parameter hybrid functional (B3LYP, which mixes Hartree-Fock and DFT exchange energy terms) (BECKE, 1993) for the exchange part, and the Lee-Yang-Parr (LYP) correlation function (LEE, et al., 1988), looking for the vibrational frequencies of the optimized structures (ALBUQUERQUE, et al., 1980). Vibrational frequencies have been calculated at B3LYP/6-311G(d,p) basis set to expand the electronic states (FAST, et al., 1999), enabling us to make the detailed IR and Raman assignments spectra of the carbidopa

molecule. All DFT calculations are obtained by performing a geometrical optimization using the GAUSSIAN 09 code (FRISCH, 2003) without any constraint on the geometry, whose convergence criteria were: maximum force smaller than 7.7×10^{-4} eV/Å; self-consistent field energy variation smaller than 2.7×10^{-5} Å; and maximum atomic displacement smaller than 3.2×10^{-5} Å.

The optical properties are analyzed through their optical absorption spectra. They were investigated by DFT calculations with LDA/PWC, GGA/PBE, and GGA/BLYP functionals, as implemented in the DMol3 program. We used only the 25 lowest singlet states to calculate the optical properties. Knowing that the carbidopa molecule has closed-shell and it is a non-periodic system, the calculations were performed using the RPA (Random Phase Approximation) method, neglecting the exchange-correlation response, but considering the electrostatic one. Gaussian integration was the broadening method used to calculate the optical spectrum with a value of 5.0 nm to the smearing width.

3 Results and discussions

The molecular conformers of carbidopa, obtained from Boltzmann jump search method of calculation, are shown in Figure 1. The carbidopa molecule contains three radicals connected to the benzene ring, being one C4O2N2H9 and the others OH hydroxyl group (GEORGE, 1989). The first radical is composed by four important groups, the so-called primary amine, secondary amine, carboxyl, and methyl. There are nine possible conformers of smaller energy for the carbidopa molecule. The carbidopa in Figure 1(a) is the conformer with the smallest energy (E = -793.66117 Ha), followed by the conformers in Figures 1(b) to 1(i), with energies in the range E = -793.65908 Ha to E = -793.64152 Ha. These energies were obtained by geometry optimized carried out on the DMol3 using DFT theory.

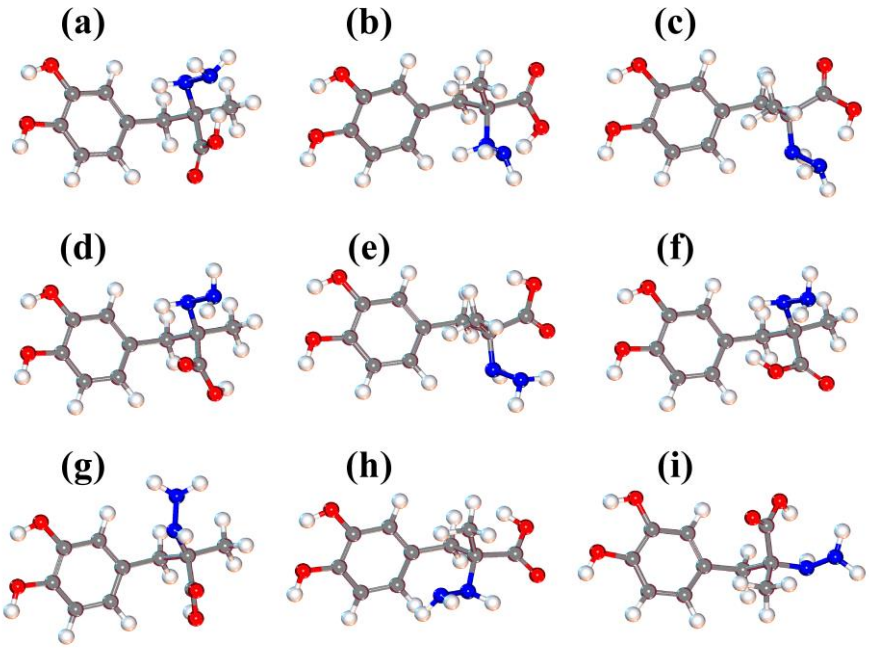

Figure 1: The carbidopa molecule conformations of smallest energy. (a) E = -793.66117 Ha, (b) E = -793.65908 Ha, (c) E = -793.65462 Ha, (d) E = -793.64962 Ha, (e) E = -793.64856 Ha, (f) E = -793.64820 Ha, (g) E = -793.64404 Ha, (h) E = -793.64237 Ha, and (i) E = -793.64152 Ha.

The geometry with the smallest energy, obtained after the quantum calculation, is the most appropriated conformer chosen to represent the carbidopa from now on. The labels adopted to identify each atom of the carbidopa optimized geometry are showed in Figure 2(a), and they are quite important to analyze their structural measures. The NHNH2 and COOH groups are positively and negatively charged, respectively. Figure 2(b) shows the projection of the calculated electron density of carbidopa onto an electrostatic potential surface. From there, one can see that the most negatively charged atoms are the one labeled as O1 and O2, followed by O3 and O4. The most positively charged atoms are the Nitrogen N5 and N6, as well as the H17, H18, H19, H20, H2, and H22 hydrogen atoms; the ring and remaining carbon atoms are slightly positively charged.

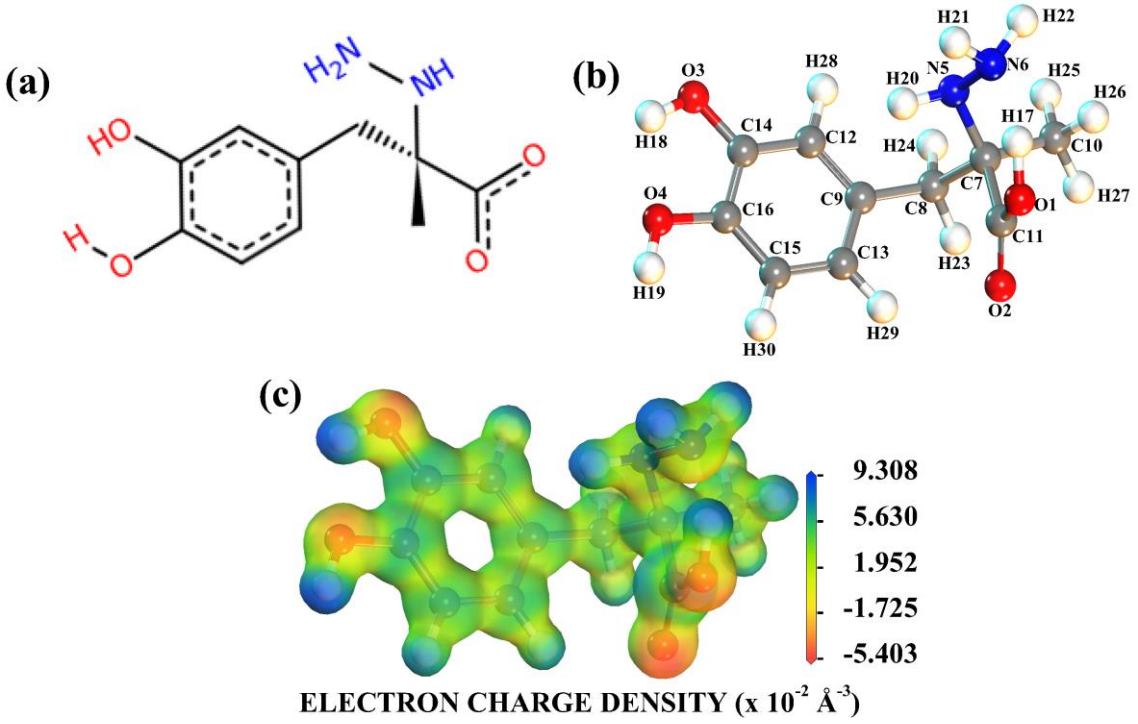

Figure 2: The carbidopa molecule of smallest energy. (a) The bonding between atoms of a molecule following the Lewis structures diagrams; (b) Its most stable converged structure; (c) The electron density of its most stable converged structure projected onto an electrostatic potential isosurface.

The optoelectonic properties depend essentially on the appropriate HOMO and LUMO energy levels and the electron and hole mobilities. It is known that (E_{gap} = $E_{(LUMO)}$ - $E_{(HOMO)}$) between the highest occupied molecular orbital (HOMO) and the lowest unoccupied molecular orbital (LUMO) is an important parameter which determines the molecular admittance because it is a measure of the electron density hardness. Calculated highest occupied molecular orbital (HOMO) and lowest unoccupied molecular orbital (LUMO) are depicted in Figure 3, while the density of states plots (DOS and PDOS) are showed in Figure 4. Analyzing the frontier region, neighboring orbitals are often closely spaced. In face of that, the consideration of only the HOMO and LUMO orbitals may not yield a realistic description of the frontier molecular orbitals (ALBUQUERQUE, et al., 2014).

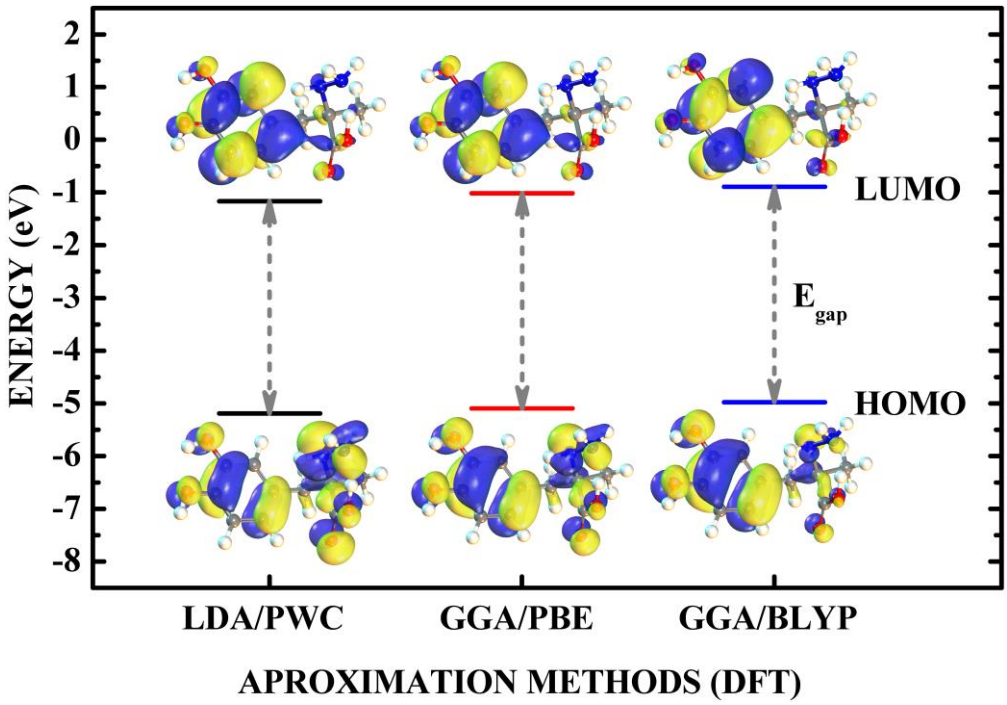

Figure 3: The highest occupied molecular orbital (HOMO) and the lowest unoccupied molecular orbital (LUMO) of the carbidopa molecule calculated by DFT-LDA/PWC, DFT-GGA/PBE, and DFT-GGA/BLYP functionals of approximation.

The total electronic density of states (DOS) were calculated using the DMol3 program (ACKLAND, 1998), that is based on a linear interpolation in parallelepipeds formed by the points of the Monkhorst-Pack set, followed by the histogram sampling of the resultant set of band energies. While the partial electronic density of states PDOS calculations are based on the Mulliken population analysis, allowing the contribution from each energy band to a given atomic orbital to be calculated.

Summation of these contributions over all bands produces a weighted DOS. In the Figure 4 one can find the respective DOS diagrams, while the inserts plots of Figure 4 are the PDOS diagrams, which show mainly the composition of the fragment orbitals contributing to the molecular orbitals. Both electronic density of states were calculated by three different quantum methods of simulation, namely the LDA/PWC, GGA/PBE, and GGA/BLYP functionals of the DFT theory. The PDOS represents useful semi qualitative tools for analyzing the electronic structure. It further qualifies these results by resolving the contributions according to the angular momentum of the states.

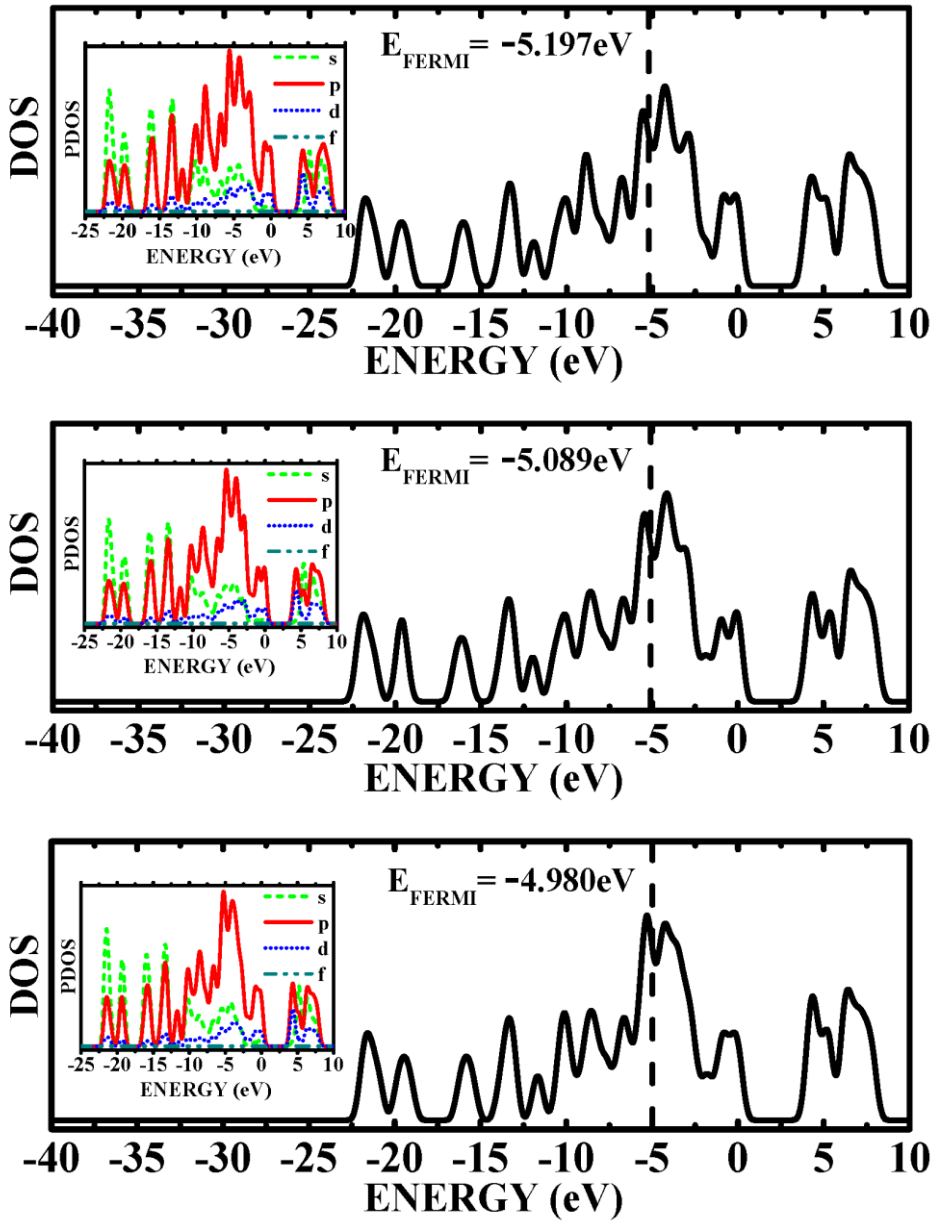

Figure 4: The predicted total electronic density of states (DOS) and partial electronic density of states (PDOS) of the carbidopa molecule calculated by DFT-LDA/PWC (top), DFT-GGA/PBE in (middle), and DFT-GGA/BLYP (bottom) functionals of approximation. The vertical dashed line on the charts indicate the Fermi energy. The labels s, p, d, and f represent the atomic orbitals.

The most relevant contribution from C, N, and O atoms to the total electronic density of states on the Fermi energy is the 2p orbital for the three kinds of calculation, with maximum at -5.633 eV (LDA/PWC), -5.388 eV (GGA/PBE), and -5.333 eV (GGA/ BLYP). As one can see on the right-hand side of Figure 4, the vertical dashed line represents the Fermi energy level,

being -5.197 eV, -5.089 eV, and -4.980 eV the value predicted by the DFT-LDA/PWC, DFT-GGA/PBE, DFT-GGA/BLYP functionals, respectively.

The energies for the HOMO, LUMO, and E_{gap} using LDA/PWC (GGA/PBE) calculation yield -5.191, -1.164, and -4.027 (-4.978, -0.891, and -4.087) eV respectively. On the other hand, using the GGA/BLYP functional, the HOMO energy is -5.098 eV, the LUMO is -1.016 eV, and the E_{gap} is -4.082 eV, respectively. The energy gap of HOMO-LUMO explains the eventual charge transfer interaction within the molecule, which influences its biological activity. Consequently, the lowering of the HOMO-LUMO band gap is essentially a consequence of the large stabilization of the LUMO due to the strong electron-acceptor ability of the electron-acceptor group. The results show that the LDA/PWC variation of energy E_{gap} gives 4.027 eV in absolute value, which is about 0.055 and 0.057 eV smaller than the GGA/PBE and GGA/BLYP DFT functionals.

We further calculate the optical absorption spectra of carbidopa using the LDA/PWC, GGA/PBE, and GGA/BLYP functionals of the DFT method. The single theoretical spectrum displayed in Figure 5 refers to the DFT/GGA/PBE functional, from which one can see the labeled peaks of resonance. It depicts six peaks of absorption, where the biggest resonance one appears at 191 nm, while the smallest one is observed at 296 nm. The remaining one are shown in the inset of Figure 5 (we kept the DFT/GGS/PBE profile for comparison), being the LDA spectrum curve dashed red, the PBE spectrum curve solid black, and the BLYP spectrum curve point-dashed blue. Looking at the LDA curve, one can notice that the peaks are shifted backward, whose second peak of resonance is less intense and more prominent when compared to the PBE spectrum, which has the second peak located at 197 nm. By contrast, in the BLYP curve the peaks are shifted forward, and the second peak disappears when it is compared to the PBE curve. The major resonance peaks in all curves are assigned between 189-194 nm, and the energy of that peak is 6.48 eV.

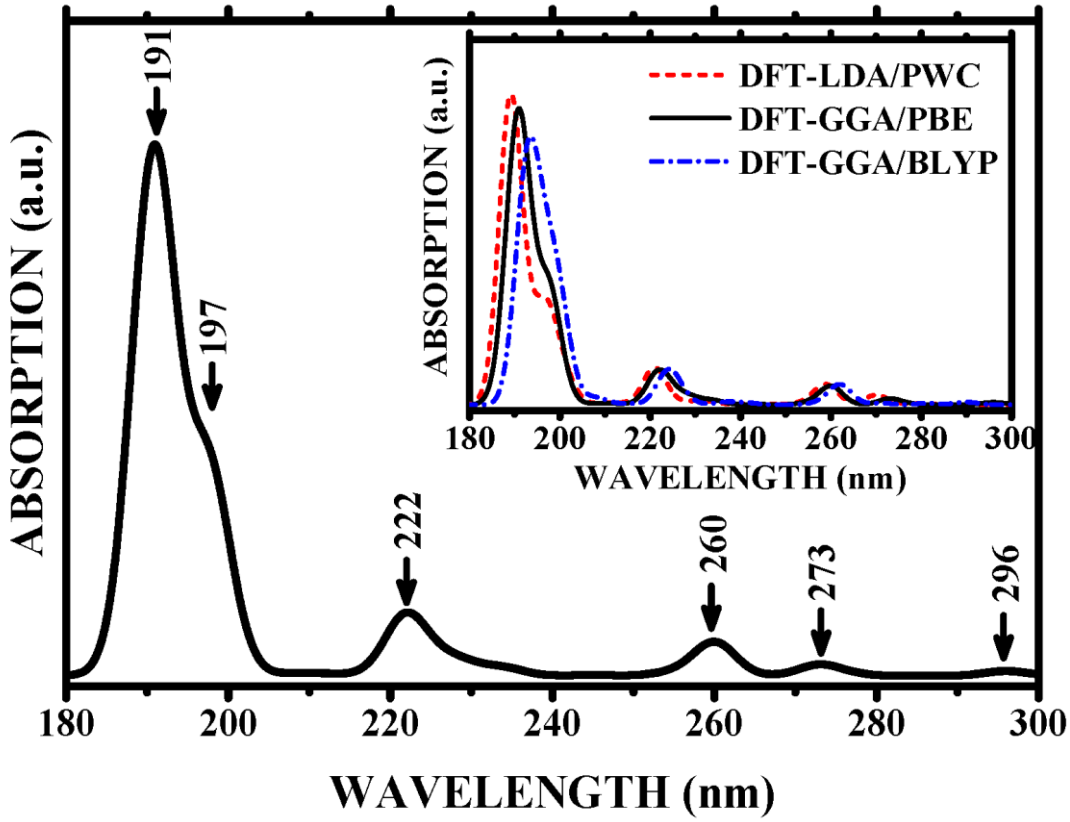

Figure 5: Optical absorption spectrum of carbidopa (with Gaussian broadening of 5.00 nm) calculated through GGA/PBE functional of DFT theory level. The peaks values of the resonance absorption peaks are labeled. The insert chart shows optical spectra calculated by LDA/PWC (dashed red line), GGA/PBE (solid black line), and GGA/BLYP (point-dashed blue line) functionals.

The carbidopa molecule consists of 30 atoms and it does not belong to any specific group of symmetry. Hence, the number of normal modes of vibrations for carbidopa is 83. Out of the 83 fundamental vibrations, 75 modes are active both by IR absorption and Raman scattering, 7 modes are active only in IR, and just 1 mode is completely Raman. The harmonic-vibrational frequencies are calculated for carbidopa through DFT/B3LYP method using the triple split valence basis set, with the diffuse and polarization functions 6-311G(d,p).

In order to show the IR and Raman peaks, we have plotted in Figures 6 and 7 the spectra profile for each kind of vibrational analysis. The IR intensity spectrum (Figure 6) related to the wavevector for each peak from 0 until 4000 cm^{-1}. The Raman scattering spectrum was built up following the same procedure of the IR curve.

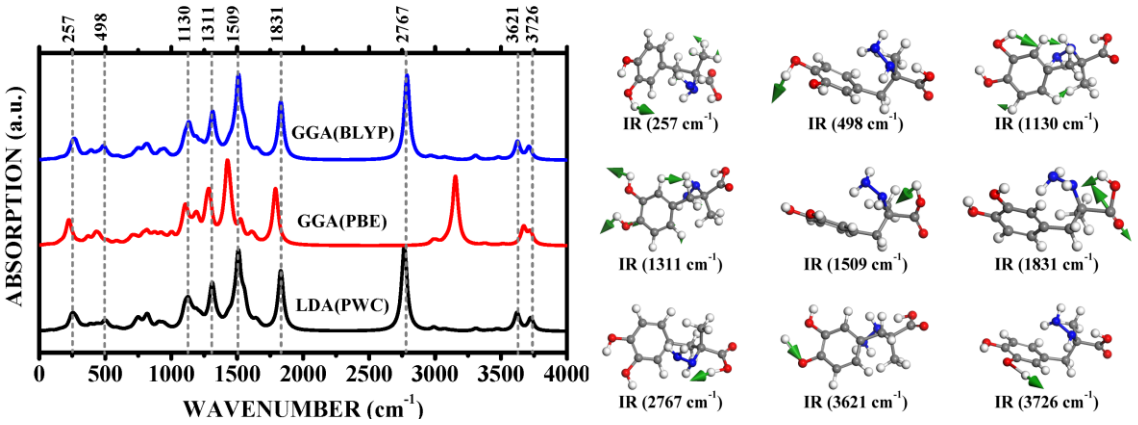

Figure 6: Theoretical calculated IR absorption spectrum of the carbidopa molecule at DFT-LDA/PWC (bottom), DFT-GGA/PBE in (middle), and DFT-GGA/BLYP (top) from 0 to 4000 cm^{-1}. On the right side are depicted nine molecular conformation and their vibrational groups for the main wavenumber peaks.

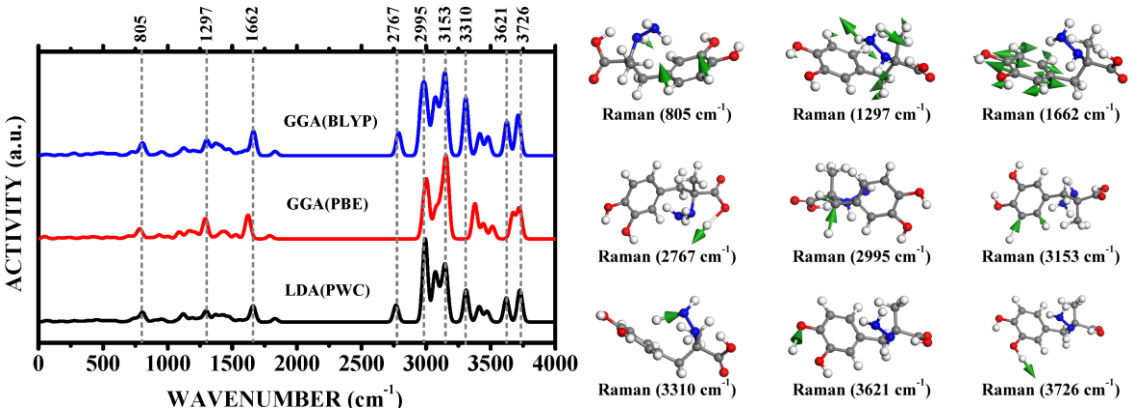

Figure 7: Same as in Figure 6 but for the calculated Raman scattering activity spectrum.

Let us analyze in depth the Raman scattering activity spectrum. To do that let us divide the group vibrations separately:

(1) the C-H vibrations: Carbidopa molecule presents the carbon-hydrogen stretching vibration in the region 3000-3100 cm^{-1}, which is a characteristic region for the aromatic compounds (HOLZE, 1992). Since carbidopa is a tri-substituted aromatic system, it has three bonds to complete the benzene ring. The expected three C-H vibrations corresponds to stretching modes of C15-H30, C12-H28, and C13-H29 bonds. These vibrations are calculated at 3150, 3180, and 3209 cm^{-1}, respectively. The C-H out-of-plane bending mode usually appears in the range 670-950 cm^{-1}, and the C-H in-plane bending vibrations in the region 950-1300 cm^{-1}. In face of that, the C-H out-of-

plane (C-H in-plane) bending vibrations are observed at 818, 882, and 950 (1168, 1181, and 1214) cm^{-1}, respectively.

(2) the C=C vibrations: The C=C stretching vibrations in aromatic compounds are observed in the region 1430-1650 cm^{-1} (KRISHNAKUMAR, et al., 2009). On the other hand, around the region 1,575-1625 cm^{-1}, the presence of conjugate, such as C=C, causes a heavy doublet formation. The six ring carbon atoms go through coupled vibrations, known as skeletal vibrations, and in the region 1420-1660 cm^{-1} they give the maximum of four bands. Because of that, the peaks at 1305, 1313, and 1357 cm^{-1} are due to the strong C-C skeletal vibrations, while the peaks at 1500, 1547, 1643, and 1661 cm^{-1} are attributed to the strong C=C stretching on the carbidopa. The peaks at 1,305, 1,313, and 1357 cm^{-1}, as well as the peaks at 1,500, 1,547, 1643, and 1661 cm^{-1} are due to the semicircle stretching and the quadrant stretching of C-C and C=C bonds, respectively. The peaks, which are assigned at 468, 552, and 589 cm^{-1}, are due to out-of-plane bending vibrations, and the peaks at 597, 674, and 755 cm^{-1} are due to C-C-C in-plane bending vibrations.

(3) the COOH vibrations: Carbonyl groups are sensitive, and both the carbon and oxygen atoms of the carbonyl move during the vibration with nearly equal amplitude. A single band was observed in the 1814 cm^{-1} position, and this is due to the C=O stretching vibration. Nevertheless, the OH stretching band is characterized by a broadband appearing near 3400 cm^{-1} (SUNDARAGANESAN, et al., 2007). The band observed at the position 3230 cm^{-1} is generated by the O-H stretching vibration. The O-H out-of-plane and in-plane bending vibrations are usually observed in the regions 590-720 cm^{-1} and 1200-1350 cm^{-1} (MAHADEVAN, et al., 2011). In carbidopa, the O-H out-of-plane and in-plane bending vibrations are found at 988 cm^{-1} and 1488 cm^{-1}, respectively. The peak in the Raman spectrum at 1244 cm^{-1}, stronger than in the IR one, is assigned to the C-O stretching mode which is a pure mode. The C-O out-of-plane and in-plane bending vibrations for carbidopa are found at 419 cm^{-1} and 755 cm^{-1}, respectively.

(4) the methyl group vibrations: The stretching vibrations on the C-H bonds of the methyl group are normally observed in the region 2,840 - 2975 cm^{-1}. In the carbidopa molecule, there is strong bands around 3034 cm^{-1} and

around 3104 cm^{-1}, corresponding to the symmetric and asymmetric stretching modes in the Raman spectrum, respectively. The CH out-of-plane and in-plane bending vibrations for CH3 methyl group in carbidopa are assigned at 755, 847, and 932 cm^{-1} and 1401, 1474, and 1492 cm^{-1}, respectively. The C-CH3 out-of-plane bending, in-plane bending, and stretching vibrations for carbidopa are found at 246, 310, and 1,114 cm^{-1}, respectively.

(5) the O-H vibrations: In a vibrational spectrum, the strength of hydrogen bond determines the position of the O-H band. Normally the O-H stretching vibrations fall in the region 3400-3600 cm^{-1} (KRISHNAKUMAR, et al., 2005). Therefore, the theoretically computed stretching values for the O-H group is 3,230, 3,788, and 3,849 cm^{-1}, whereas the O-H out-of-plane and in-plane bending modes are observed at 1,643, 1,661, 1,814 cm^{-1} and 242, 459, 988 cm^{-1}, respectively, as pure mode of bending vibration. The two last peaks in the Raman spectrum are related with the stretching on the O-H group linked to the phenyl ring.

(6) the NHNH2 vibrations: The H-N stretching modes are more visible in the Raman activities spectrum, being localized around 3500 cm^{-1}. The NH2 symmetric and asymmetric stretching is observed at 3476 and 3553 cm^{-1}, respectivelly. The H atom of the H-N-N group, presents stretching vibration at 3512 cm^{-1} and the N-N stretching is seen at 1017 cm^{-1}. By contrast, the rocking mode is assigned in the range 28 and 43 cm^{-1}; the wagging mode is found in the range 1099-1175 cm^{-1}; and the twisting vibration mode is observed from 1279 to 1356 cm^{-1}. The carbidopa compound presents two joined N nitrogen atoms. Therefore, there is a N-N stretching vibration mode on that molecule, being observed at 1017 cm^{-1}, while the C-N stretching vibration appears at 1175 cm^{-1}.

4 Conclusions

To summarize, we have performed a quantum chemical study of carbidopa using first-principle DFT approaches within the LDA/PWC, GGA/PBE, and GGA/BLYP exchange-correlation functionals. After carrying out a search for its optimal structure, we took into account the conformation of smallest energy

(-793.66117 eV), from one of the nine geometries of smaller energies considered.

We calculated the HOMO and LUMO molecular orbital to study the frontier orbitals. In average, the HOMO energy was about -5.089 eV, and the LUMO energy about -1.024 eV, giving ∆(HOMO-LUMO) equal to -4.065 eV, all of them predicted by the three different DFT functional approaches. To confirm these results, the total (DOS) and the partial (PDOS) electronic density of states were analyzed. Besides, the Fermi energy level is -0.188 eV in average and the simulation predicted a density of states different of zero on the Fermi level. Meanwhile, observing the PDOS curves, one can realize that the most relevant contribution to the DOS was given by the 2p atomic orbital.

The carbidopa conformer of smallest energy was also optimized using the B3LYP exchange-correlation functional and 6-311G(d,p) basis set to calculate their infrared intensity and Raman activity spectra, as well as to analyze its frequency assignments. From that, the exact identity of the carbidopa molecule was established, following a description which show, for instance, where absorption by single and double bonds are observed in the IR and Raman spectra, considering their most important vibration groups, namely: C-H, C=C, COOH, the methyl group, the O-H, and the NHNH2. The calculated vibrational modes proved that the carbidopa molecule is stable (no imaginary frequency). Furthermore, one can identify that a very strong absorption peak, at 3230 cm^{-1} (IR intensity), is related to the H17- O1 stretching vibration mode of the carboxyl group. On the other hand, the calculated Raman activity spectrum exhibits the most intense peak at 3035 cm^{-1}, corresponding to the H-C symmetric stretching mode of the methyl group.

We strongly hope that, motivated by these and other progress, the theoretical predictions obtained here can be reproduced experimentally and that experimentalists get encouraged to face them.

5 References

LLOYD, K. et al. Parkinson's Disease: Activity of L-Dopa Decarboxylase in Discrete Brain Regions, **Science**, v. 170, n. 3963, 1970. Available in: <http://dx.doi.org/10.1126/science.170.3963.1212>. Access in: April 12, 2017.

ABOU-SLEIMAN, P. M. et al. Expanding insights of mitochondrial dysfunction in Parkinson's disease, **Nature Reviews Neuroscience**, v. 7, n. 3, 2006. Available in: < https://doi.org/10.1038/nrn1868>. Access in: April 12, 2017.

SCHAPIRA, A. H. V. et al. Timing of treatment initiation in Parkinson's disease: A need for reappraisal?, **Annals of Neurology**, v. 59, n. 3, 2006. Available in: <http://dx.doi.org/10.1002/ana.20789>. Access in: April 12, 2017.

CALNE, D. B. Treatment of Parkinson's Disease, **New England Journal of Medicine,** v. 329, n. 14, 1993. Available in: <http://dx.doi.org/10.1056/NEJM199309 303291408>. Access in: April 12, 2017.

HUTTON, J. et al. Treatment of chronic Parkinson's disease with controlled-release carbidopa/levodopa, **Archives of Neurology**, v. 45, n. 8, 1988. Available in: <http:// dx.doi.org/10.1001/archneur.1988.00520320047014>. Access in: April 12, 2017.

FRAZÃO, N. F. et al. Four-level levodopa adsorption on C60 fullerene for transdermal and oral administration: a computational study, **The Royal Society of Chemistry Advances**, v. 2, n. 22, 2012. Available in: <http://dx.doi.org/10.1039/C2RA20606D>. Access in: April 12, 2017.

DELLEY, B. From molecules to solids with the DMol3 approach, **The Journal of Chemical Physics**, v. 113, n. 18, 2000. Available in: <http://dx.doi.org/10.1063/1.1316015>. Access in: April 12, 2017.

HOHENBERG, P. et al. Inhomogeneous Electron Gas, **Physical Review B**, v. 136, n. 3, 1964. Available in: <https://doi.org/10.1103/PhysRev.136.B864>. Access in: April 13, 2017.

KOHN, W. et al. Self-Consistent Equations Including Exchange and Correlation Effects, **Physical Review A**, v. 140, n. 4, 1965. Available in: <https://doi.org/10.1103/PhysRev.140.A1133>. Access in: April 13, 2017.

JONES, R. O. et al. The density functional formalism, its applications and prospects, **Reviews of Modern Physics**, v. 61, n. 3, 1989. Available in: <https://doi.org/10.1103/RevModPhys.61.689>. Access in: April 13, 2017.

DAL CORSO, A. et al. Generalized-gradient approximations to density-functional theory: A comparative study for atoms and solids, **Physical Review B**, v. 53, n. 3, 1996. Available in: <https://doi.org/10.1103/PhysRevB.53.1180>. Access in: April 13, 2017.

PERDEW, J. P. et al. Accurate and simple analytic representation of the electron-gas correlation energy, **Physical Review B**, v. 45, n. 23, 1992. Available in: <https://doi.org/10.1103/PhysRevB.45.13244>. Access in: April 13, 2017.

PERDEW, J. P. et al. Accurate and simple density functional for the electronic exchange energy: Generalized gradient approximation, **Physical Review B**, v. 33, n. 12, 1986. Available in: <https://doi.org/10.1103/PhysRevB.33.8800>. Access in: April 13, 2017.

PERDEW, J. P. et al. Generalized Gradient Approximation Made Simple, **Physical Review Letter**, v. 77, n. 18, 1996. Available in: <https://doi.org/10.1103/PhysRevLett.77.3865>. Access in: April 13, 2017.

BECKE, A. D. A multicenter numerical integration scheme for polyatomic molecules. **Journal of Chemical Physics**, v. 88, n. 4, 1988. Available in: <http://dx.doi.org/10.1063/1.454033>. Access in: April 13, 2017.

BECKE, A. D. Density-functional thermochemistry. III. The role of exact exchange, **Journal of Chemical Physics**, v. 98, n. 7, 1993. Available in: <http://dx.doi.org./10.1063/1.464913>. Access in: April 13, 2017.

HENRIQUES, J. M. et al. Vibrational and thermodynamic properties of orthorhombic CaSnO3 from DFT and DFPT calculations, **Journal of Physics and Chemistry of Solids**, v. 77, n. x, 2015. Available in: <http://dx.doi.org/10.1016/j.jpcs.2014.09.016>. Access in: April 14, 2017.

FRAZÃO, N. F. et al. Conformational, Optoelectronic and Vibrational Properties of the Entacapone Molecule: A Quantum Chemistry Study, **Journal of Nanoscience and Nanotechnology**, v. 16, n. 5, 2016. Available in: <http://dx.doi.org/ 10.1166/jnn.2016.12382>. Access in: April 14, 2017.

LEE, C. et al. Development of the Colle-Salvetti correlation-energy formula into a functional of the electron density, **Physical Review B**, v. 37 n. 2, 1988. Available in: <https://doi.org/10.1103/PhysRevB.37.785>. Access in: April 15, 2017.

ALBUQUERQUE, E. L., et al. Theory of Brillouin Scattering by Love Waves, **Journal of Physics C: Solid State Physics**, v. 13, n. 9, 1980. Available in: <https://doi.org/10.1088/0022-3719/13/9/023>. Access in: April 15, 2017.

FAST, P.L. et al. Optimized Parameters for Scaling Correlation Energy, **Journal Physical Chemistry. A**, v. 103, n. 17, 1999. Available in: <https://doi.org/10.1021/jp9900382>. Access in: April 15, 2017.

FRISCH, M. J. et al, Gaussian 03, **Gaussian, Inc.**, Wallingford, CT, 2003. Available in: <http://gaussian.com/g03citation/>. Access in: April 15, 2017.

GEORGE, P. A test of the AM1 model for calculating energies and structural-properties of benzene, toluene, naphthalene, 1-methyl and 2-methylnaphthalene, Tetrahedron, v. 45, n. 3, 1989. Available in: <https://doi.org/10.1016/0040-4020(89)80088-2>. Access in: April 15, 2017.

ALBUQUERQUE, E. L. et al. DNA-based nanobiostructured devices: The role of quasiperiodicity and correlation effects, **Physics Reports**, v. 535, n. 4, 2014. Available in: <http://doi.org/10.1016/j.physrep.2013.10.004>. Access in: April 15, 2017.

ACKLAND, G. J. Embrittlement and the Bistable Crystal Structure of Zirconium Hydride, **Physical Review Letter**, v. 80, n. 10, 1998. Available in: <https://doi.org/10.1103/PhysRevLett.80.2233>. Access in: April 15, 2017.

HOLZE, R. Spectroelectrochemical studies of the adsorption of 4-dimethylamino-4'-nitrostilbene on silver and gold electrodes, Vibrational Spectroscopy, v. 3, n. 4, 1992. Available in: <https://doi.org/10.1016/0924-2031(92)85001-H>. Access in: April 15, 2017.

KRISHNAKUMAR, V. et al. Scaled quantum chemical studies on the vibrational spectra of 4-bromo benzonitrile, **Spectrochimica Acta Part A: Molecular and Biomolecular Spectroscopy**, v. 71, n. 5, 2009. Available in: <http://doi.org/10.1016/j.saa.2008.06.037>. Access in: April 15, 2017.

SUNDARAGANESAN, N. et al. Vibrational spectra and assignments of 5-amino-2-chlorobenzoic acid by ab initio Hartree–Fock and density functional methods, **Spectrochimica Acta Part A: Molecular and Biomolecular Spectroscopy**, v. 66, n. x, 2007. Available in: <http://doi.org/10.1016/j.saa.2006.03.008>. Access in: April 15, 2017.

MAHADEVAN, D. et al. Vibrational spectroscopy (FTIR and FTRaman) investigation using ab initio (HF) and DFT (B3LYP) calculations on the structure of 3-Bromo phenol, **Spectrochimica Acta Part A: Molecular and Biomolecular Spectroscopy**, v. 78, n. 2, 2011. Available in: <http://doi.org/10.1016/j.saa.2010.11.025>. Access in: April 15, 2017.

KRISHNAKUMAR, V. et al. Vibrational spectra and potential energy distributions for 4,5-dichloro-3-hydroxypyridazine by density functional theory and normal coordinate calculations, **Spectrochimica Acta Part A: Molecular and Biomolecular Spectroscopy**, v. 61, n. 11-12, 2005. Available in: <http://doi.org/10.1016/j.saa.2004.08.027>. Access in: April 15, 2017.